STUDY OF PRISTINE CARBON NANOTUBE UNDER TENSILE AND COMPRESSIVE LOADS USING MOLECULAR DYNAMICS SIMULATION

S. N. Hossain Rubaiyat[1] and Sanjib Chandra Chowdhury[2,*]
[1]Department of Mechanical Engineering, Military Institute of Science and Technology, Dhaka
[2]Department of Mechanical Engineering, Bangladesh University of Engineering & Technology, Dhaka.
*Corresponding email: sanjib@me.buet.ac.bd

Abstract: *After the discovery, carbon nanotubes (CNTs) have received tremendous scientific and industrial interests. This is due to their exceptional mechanical, electrical, and thermal properties. CNTs having pristine structure (i.e., structure without any defect) hold very high mechanical properties. In this article, mechanical properties of CNTs are studied under both tensile and compressive loads using molecular dynamics (MD) simulations. Four armchair single-walled nanotubes (SWNTs) having indexes of (3,3), (4,4), (5,5) and (6,6) with pristine structure are simulated with MD. Molecular simulations are carried out using the classical MD method, in which the Newtonian equations of motion are solved numerically for a set of atoms. The velocity-Verlet algorithm is used for solving the Newtonian equations of motion. The Brenner potential is used for carbon-carbon interaction in the CNT and temperature of the system is controlled by velocity scaling. Simulation results show that modulus of elasticity of CNTs varies significantly with CNT diameter. The results obtained from the compressive test by MD simulations are in well agreement with the results obtained from theoretical Euler equation and parabolic equation for long and short column respectively.*

Keywords: *Carbon nanotubes; Molecular dynamics; Young's modulus; Failure strength; Failure strain.*

INTRODUCTION

Carbon Nanotubes (CNTs) can be considered as long wrapped graphene sheets[1]. Since their discovery by Iijima[2] in 1991, CNTs have received tremendous scientific and industrial interests. This is due to their exceptional mechanical, electrical, and thermal properties. CNTs can be seen as dream materials whose Young's modulus and tensile strength are in the order of 1000 GPa and 200 GPa, respectively[3]. Research on CNTs has received much attention during the last ten years due to its large aspect ratio and mechanical properties. The early studies concerned the mechanical properties of CNTs are mainly focused on single-walled nanotubes (SWNTs) under axial compression[4-11]. Among these studies, Yakobson et al.[4] first investigated the instability of SWNTs under axial compression, bending and torsional deformation. In their study, a continuum shell model was also introduced to describe the buckling and bending behaviors of CNTs in plastic deformation regime by properly chosen parameters. In contrast to the CNTs under axial compression, studies on CNTs under axial tension are limited; only a few has been reported on the plastic properties of CNTs under large tensile strain. Yakobson et al.[12] studied the behavior of CNTs under higher tension using Tersoff- Brenner's reactive empirical bond-order (REBO) potential[13-15]. Large elastic deformations of CNTs under axial tension, axial compression, and torsion were investigated in their work. Xiao and Liao[16] simulated the nonlinear elastic properties of CNTs under axial tensile deformation

Nomenclature

B^*_{ij}	Many body coupling between the bond from atom *i* to atom *j*
d	Diameter of the CNT
E_{tot}	Total potential energy
$f(r)$	Cut-off function
F	Axial force
F_1	Total axial inter atomic force of the rigidly moving end atoms at corresponding strain
F_0	Total axial inter atomic force of the rigidly moving end atoms at zero strain
$G_c(\theta_{ijk})$	Function of the angle between bonds *i-j* and *i-k*
h	Thickness of the CNT
L_0	Initial length of the CNT
L_1	Current length of the CNT
r_{ij}	Bond length between atom *i* and atom *j*
s	Cross sectional area of CNT
$V_R(r_{ij})$	Pair-additive repulsive interactions
$V_A(r_{ij})$	Pair-additive attractive interactions
ε	Axial strain
σ	Axial stress
D_e, S, β, R_e, a_0, c_0, d_0, R_1, R_2	Brenner Parameters

using the second generation Brenner potential.

Experimental work on measuring the mechanical properties of CNTs under tension is limited. Yu et al.[17] measured the tensile strengths of multi-walled CNTs. The stress–strain curve was obtained and analyzed for Young's modulus of individual multi-walled CNTs. Their experimental work revealed that the breakage first takes place at the outermost layer of the multi-walled CNTs. Bozovic et. al [18] have used the atomic force microscope tip to induce varying degrees of strain in the SWNTs. Their experimental results showed that SWNTs can sustain elongations as large as 30% without breaking. There are very few research works regarding the mechanical properties characterization of CNTs of different diameter. As CNTs can be of different diameter, it is necessary to investigate the diameter effect on their mechanical properties. Due to high strength and stiffness, CNTs are ideal candidate for reinforcement of various materials specially polymers. Having high strength and stiffness along with better thermal and electric properties, CNTs are used in making nano-devises/nanostructure like nano-probe for nano-scale metrology, micro- and nano-electronics, sensors, actuators, field emitters etc. Thus it is necessary to know the behavior of CNT under tensile and compressive loads for designing CNT based devices in these fields.

In this paper, we investigate the mechanical behavior of SWNTs of different diameter under tensile and compressive loads using MD simulations. From our simulations, we obtain the stress-strain relationship to describe the elastic and plastic behaviors of SWNTs for both tensile and compressive loads. We also compute the mechanical properties, such as Young's modulus, yield strength, ultimate strength, failure strength and failure strain. Results obtained from our simulation for compressive tests are compared with results obtained from theoretical Euler equation and parabolic equation for long and short column respectively.

MOLECULAR DYNAMICS METHOD

In this work, molecular simulations are performed to investigate the mechanical behavior of pristine SWNTs. At first, SWNT structure is generated with known coordinate of each carbon atom. Then molecular simulation is carried out using the classical MD method[19], in which the Newtonian equations of motion are solved numerically for a set of atoms. The velocity-Verlet algorithm[20] is used for solving the Newtonian equations of motion. To control the temperature, velocity scaling is used. The Brenner potential[15] is used for carbon-carbon interaction in the CNT. Atoms of two rings of both ends of the nanotube are moved rigidly with incremental displacement in outward and inward direction for tension and compression, respectively. Applied force is calculated by calculating the inter-atomic force of the atoms of the two rings of any end.

Potential Functions and Parameters

The Brenner potential function[15], which is used for carbon-carbon interaction in the CNT, is given as

$$E_{tot} = \sum_i \sum_{j(<i)} \{V_R(r_{ij}) - B^*_{ij} V_A(r_{ij})\} . \quad (1)$$

Where r_{ij} is the length of the bond between atom i and atom j (Fig.1). Here,

$$V_R(r) = f(r)\frac{D_e}{S-1}\exp\left\{-\beta\sqrt{2S}(r-R_e)\right\}, \quad (2)$$

$$V_A(r) = f(r)\frac{D_e S}{S-1}\exp\left\{-\beta\sqrt{\frac{2}{S}}(r-R_e)\right\}, \quad (3)$$

$$B^*_{ij} = \frac{B_{ij}+B_{ji}}{2},$$

$$B_{ij} = \left[1+\sum_{k\neq i,j}\{G_c(\theta_{ijk})f(r_{ik})\}\right]^{-\delta} . \quad (4)$$

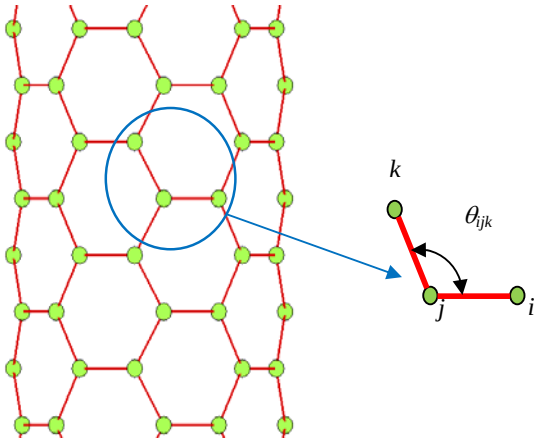

Figure 1. Orientation of carbon atoms in a CNT structure.

In Eq. (4), $G_c(\theta_{ijk})$ function is given by

$$G_c(\theta_{ijk}) = a_0\left(1+\frac{c_0^2}{d_0^2}-\frac{c_0^2}{d_0^2+(1+\cos\theta_{ijk})^2}\right), \quad (5)$$

and $f(r)$ value is as follows

$$f(r) = \begin{cases} 1 & r < R_1 \\ \frac{1}{2}+\frac{1}{2}\cos\left\{\frac{\pi(r-R_1)}{(R_2-R_1)}\right\} & R_1 < r < R_2 \\ 0 & r > R_2 \end{cases} . \quad (6)$$

Brenner[15] has proposed two sets of potential parameters. The first set of parameters which are adapted here is shown below:

D_e=6.325 eV	S=1.29	β=0.15 nm
R_e=0.1315 nm,	a_0= 0.11304	c_0=19
d_0=2.5	R_1=0.195 nm,	R_2=0.2 nm.

Tensile and Compressive Test Procedure

Atomistic model of the tensile and compressive tests of SWNT is shown in Fig. 2 and Fig. 3, respectively. In the MD simulation, the atoms of two rings of both ends of the nanotube are moved rigidly with incremental displacement of 0.0005 nm outward and inward for tensile and compressive tests, respectively. Each incremental displacement of the CNT is followed by the conjugate energy minimization method and 100 numbers of molecular dynamics steps for equilibration of the system. In MD simulations, time step of 0.1 fs is considered to solve the equations of motion using velocity-Verlet algorithm. The temperature of the system is kept constant at 300 K and controlled by velocity scaling. During the equilibration period, ends atoms are kept fixed in plane. Stress is calculated using the following formula:

$$\sigma = \frac{F}{s}. \quad (7)$$

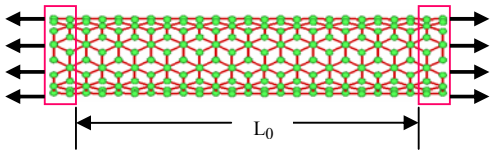

Figure 2. Atomistic model for tensile test.

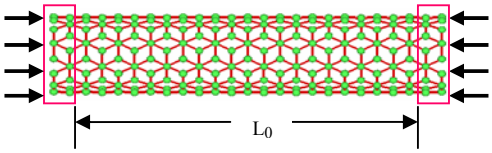

Figure 3. Atomistic model for compressive test.

The axial force $F = F_1 - F_0$ and cross-sectional area (Fig. 4) $s = \pi dh$. Here h= 0.34 nm is used. Strain is calculated according to the following formula:

$$\varepsilon = \frac{L_1 - L_0}{L_1}. \quad (8)$$

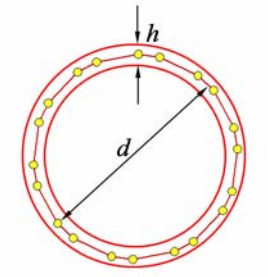

Figure 4. Cross section of a SWNT.

RESULTS AND DISCUSSIONS

To examine the mechanical properties of nanotube, tensile and compressive tests of (3,3), (4,4), (5,5) and (6,6) armchair SWNTs are conducted using MD simulations. For tensile test, length of 7.45 nm and for compressive test aspect ratios of 4-20 are considered for all types of SWNTs. Failure strength, failure strain, yield strength and modulus of elasticity for tensile and compressive loads are calculated. Failure behaviors of nanotubes under tensile and compressive loads are also examined.

Validation of the MD Code

In order to validate the present MD simulation code, the tensile stress–strain response is simulated for a (7,7) SWNT with a length-to-diameter ratio, *l/d*=8. The results of the current simulation is compared with the results of Yeak et al.[21] as depicted in Fig. 5 (a). It is observed that the present simulation stress–strain results deviate slightly from the results of Yeak et al. The present simulation results yield a slightly higher failure strain and failure stress because of the different values of Brenner potential parameters used in the simulations. The change in the values of the Brenner potential parameters has no effect on the stress-strain response at relatively smaller strain. However, they affect on the stress-strain relationship at higher strain. It is seen that if the values of Brenner parameter, R_1 and R_2[15] change the failure stress and strain also change (Fig. 5(b)). Since the Young's modulus and failure behavior of the CNTs are the main concern of present study, the maximum values of R_1 and R_2 [22] are considered.

Tensile Test of SWNTs

The stress-strain curves of (3,3), (4,4), (5,5), and (6,6) pristine SWNT are presented in Fig. 6. It is found from the figure that the SWNT does not have a well defined yield point. Since there is no well defined yield point, therefore yield strength is calculated by offset method. The yield strength is calculated at 0.2% strain. The average yield strength found for different diameter SWNTs is about 103 GPa. The snap shot of SWNT for tensile test at different strains are shown in Fig. 7. When SWNT is loaded above the yield strength, it begins to 'neck' (Fig. 7(b)) as the cross sectional area of the nanotube decreases due to plastic flow. From the stress-strain curves of SWNT, it is seen that the ultimate strength and failure strength are the same which is the character of typical brittle materials. The Young's modulus of elasticity is calculated from the slope of the stress-strain curve. The variation of Young's modulus with diameter is presented in Fig. 8. It is found that the Young's modulus varies significantly with diameter. The Young's modulus increases as the diameter increases. The lower young modulus at smaller

nanotube diameter is attributed to the higher curvature, which results in a more significant distortion of C-C bonds in the CNT. The variation of failure stress and failure strain with diameter is illustrated in Fig. 9 and Fig. 10 respectively. It is seen that the variation of the failure stresses and failure strains with the diameter of the SWNTs is negligible. The failure strength and failure strain do not depend on curvature, rather depend on the C-C bond strength and strain. For this reason, failure strength and strain are independent of tube diameter. The failure stress and failure strain decrease only by 1.3% and 4.23% respectively with the increase of diameter by 233%.

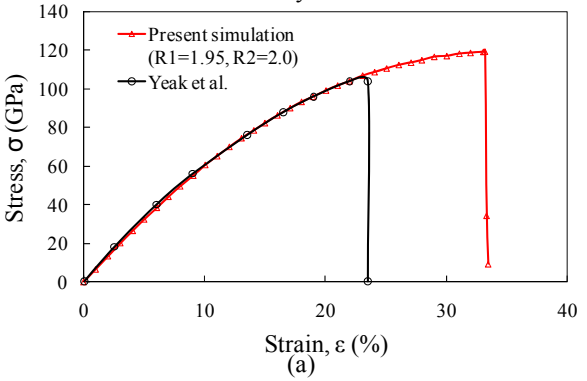

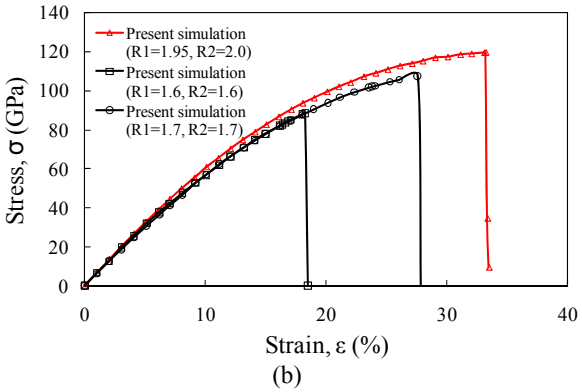

Figure 5. Stress-strain behavior of a (7,7) SWNT under axial tension; (a) comparison with literature, (b) effect of potential parameters R_1 & R_2.

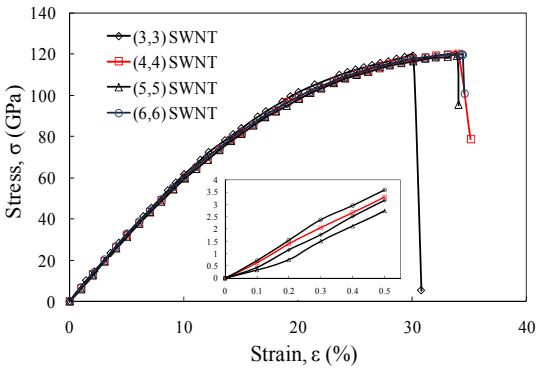

Figure 6. Tensile stress versus strain curve for SWNTs.

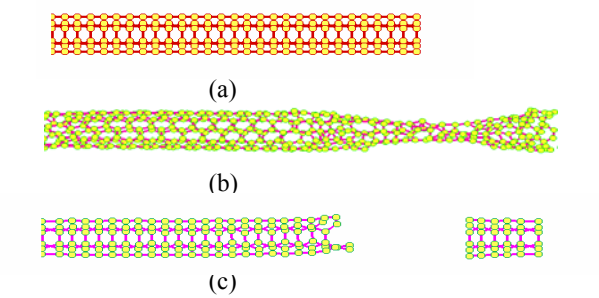

Figure 7. Snap shot of tensile test of (5,5) pristine SWNT; (a) at 0% strain, (b) at 18% strain (necking), (c) failure at 34% strain.

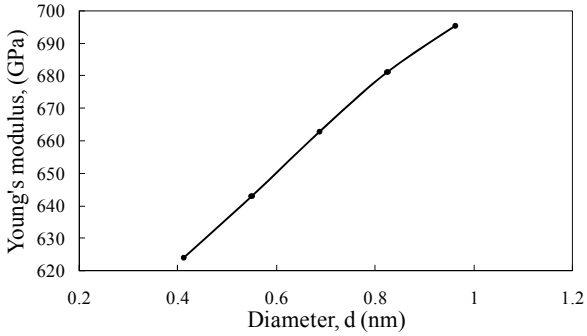

Figure 8. Young's modulus versus diameter curve for pristine SWNT under tensile load.

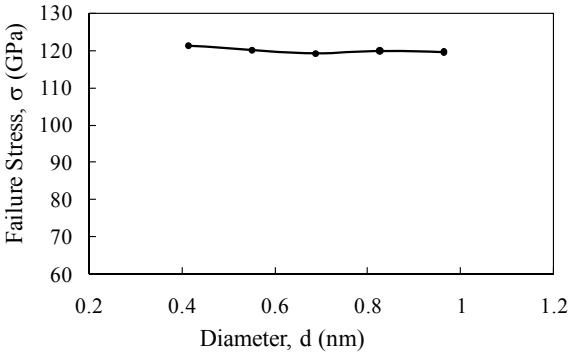

Figure 9. Failure stress versus diameter for pristine SWNT under tensile load.

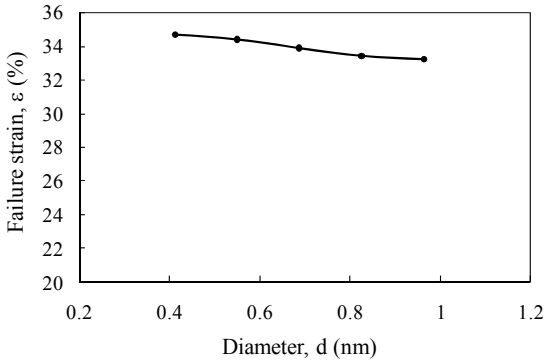

Figure 10. Failure strain versus diameter curve for pristine SWNT under tensile load.

Compressive Test of SWNTs

Like tensile tests, compressive tests are also performed for SWNTs with various diameters. The end condition of the CNTs for the simulation used is fixed-fixed. The stress-strain curves of (3,3), (4,4), (5,5) and (6,6) pristine SWNT under compressive loads are presented in Fig. 11. The nature of the stress-strain curve of SWNT under compressive load is almost similar to that of stress-strain curve under tensile load. The Young's modulus is calculated from the slope of the stress-strain curve under compressive load. For CNT with specific diameter, Young's modulus in compressive test is found almost the same as that found in the tensile test. The variation of Young's modulus with diameter is presented in Fig. 12. It is seen from the figure that Young's modulus increases as the diameter increases.

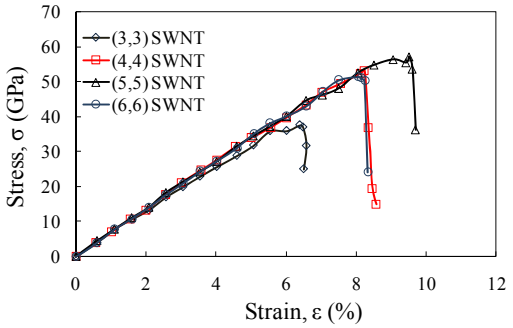

Figure 11. Compressive stress versus strain curve for SWNTs.

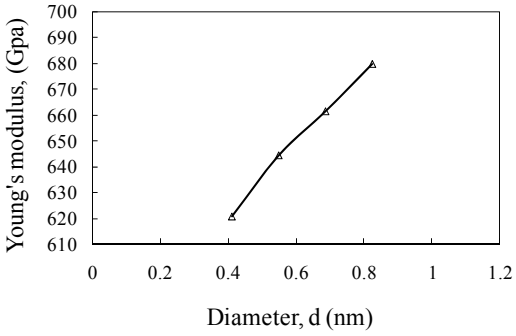

Figure 12. Young's modulus versus diameter curve for pristine SWNT under compressive load.

The critical stress (i.e. failure stress) versus slenderness ratio curve is presented in Figs. 13 to 16. The results obtained from MD simulations are compared with results obtained from theoretical parabolic and Euler equation. The comparisons are also presented in these figures. Critical slenderness ratio of particular CNT is calculated at half of the corresponding yield strength using the Euler equation for column. Based on the critical slenderness ratio, the columns are divided as short column and long column. From these figures it is clear that MD simulation results are in well agreement with those of theoretical parabolic equation for short columns and theoretical Euler equation for long columns.

During the compressive tests deformation patterns of SWNTs with different slenderness ratios are observed. Two types of deformations namely crushing (or kinking) and buckling are found for different slenderness ratios of SWNT and these are shown in Fig. 17 and Fig. 18. It is observed that crushing occurs at lower slenderness ratio whereas buckling is found at higher slenderness ratio.

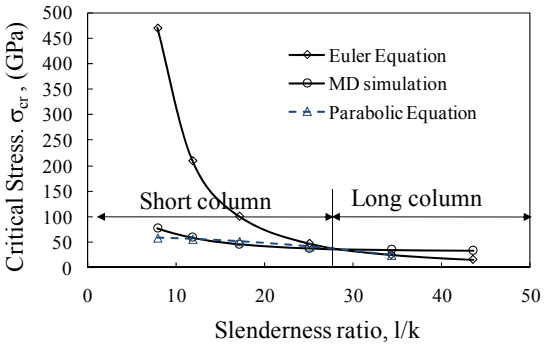

Figure 13. Critical stress versus slenderness ratio curve for (3,3) SWNT.

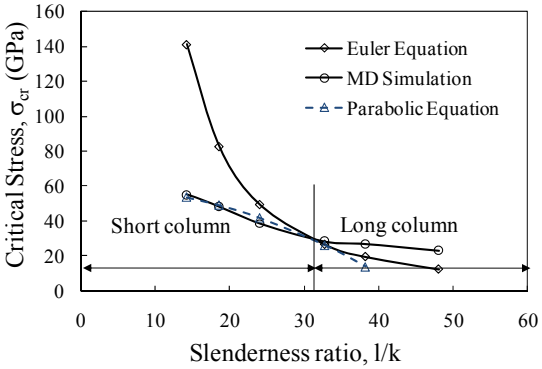

Figure 14. Critical stress versus slenderness ratio curve for (4,4) SWNT.

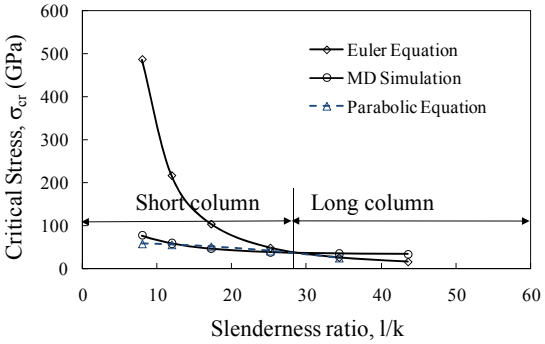

Figure 15. Critical stress versus slenderness ratio curve for (5,5) SWNT.

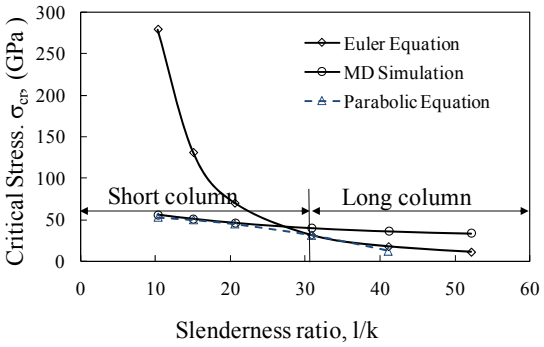

Figure 16. Critical stress versus slenderness ratio curve for (6,6) SWNT.

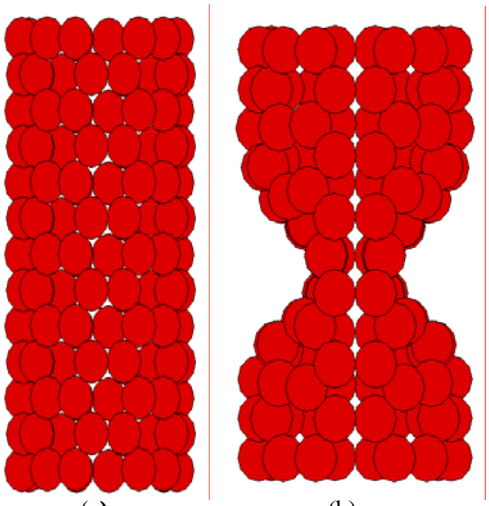

Figure 17. Snapshot of (5,5) SWNT with slenderness ratio, l/k=10.13 under compressive load; a) undeformed, b) crushing (or kinking).

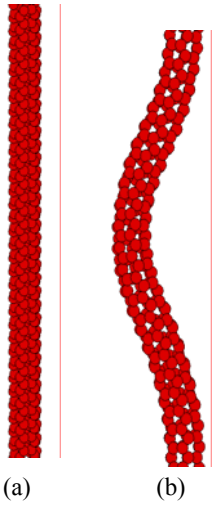

Figure 18. Snapshot of (3,3) SWNT with slenderness ratio l/k=43.57 under compressive load; a) undeformed, b) buckling.

CONCLUSIONS

In this paper, MD simulation for armchair SWNTs under axial tensile and compressive loads is carried out. From simulations, the stress-strain relationship to describe the elastic and plastic behaviors of SWNTs for both tensile and compressive loads is obtained. The mechanical properties, such as Young's modulus, yield strength, ultimate strength, failure strength and failure strain are also computed. From the simulation, the following conclusions are drawn:

- SWNTs have no well defined yield strength.
- The ultimate strength and failure strength are found as the same.
- Young's modulus is a strong function of diameter of SWNTs and diameter has no significant effect on failure strength and failure strain of SWNTs.
- The results obtained from the compressive test by MD simulations are in well agreement with the results obtained from theoretical Euler equation and parabolic equation for long and short column respectively.

REFERENCES

[1] Dresselhaus, G., Saito, R., Dresselhaus, M. S., 1999, "Physical Properties of Carbon Nanotubes," Imperial College Press, USA.

[2] Iijima, S., 1991, "Helical microtubules of graphite carbon," Nature, 354, pp.56–58.

[3] Lau, K. T., Hui, D., 2002 "The revolutionary creation of new advanced materials-carbon nanotube composites," Compos Part B, vol. 33, pp. 263–277.

[4] Yakobson, B. I., Brabec C. J., Bernholc, J., 1996 "Nanomechanics of carbon tubes: instabilities beyond linear response," Phys Rev Lett., vol.76: pp. 2511–2514.

[5] Garg, A., Han, J., Sinnott S. B., 1998, "Interactions of carbon-nanotubule proximal probe tips with diamond and graphene," Phys Rev Lett., vol. 81, pp. 2260–2263.

[6] Hertel, T., Walkup, R. E., Avouris, P., 1998, "Deformation of carbon nanotubes by surface van der Waals forces," Phys Rev B, vol. 58, pp. 13870–13873.

[7] Liew, K. M., Wong, C. H., He, X. Q., Tan, M. J., Meguid, S. E., 2004, "Nanomechanics of single and multi-walled carbon nanotubes," Phys Rev B, vol. 69, pp. 1154-1157.

[8] Ru, C. Q., 2000,"Elastic buckling of single-walled carbon nanotube ropes under high

pressure," Phys Rev B, vol. 62, pp.10405–10408.

[9] Ru, C. Q., 2000, "Effect of van der Waals forces on axial buckling of a double-walled carbon nanotube," J Appl Phys, 87, pp. 7227–7231.

[10] Lourie, O., Cox, D. M., Wagner, H. D., 1998, "Buckling and collapse of embedded carbon nanotubes," Phys Rev Lett., vol. 81, pp. 1638–1641.

[11] Srivastava, D., Menon, M., Cho, K., 1999, "Nanoplasticity of single-wall carbon nanotubes under uniaxial compression," Phys Rev Lett, vol. 83, pp. 2973–2986.

[12] Yakobson, B. I., Campbell, M. P., Brabec, C. J., Bernholc J., 1997, "High strain rate fracture and C-chain unraveling in carbon nanotubes," Comp Mater Sci, 8, pp.341–348.

[13] Tersoff, J., 1986, "New empirical model for the structural properties of silicon," Phys Rev Lett, vol. 56, pp. 632–635.

[14] Tersoff, J., 1988, "New empirical approach for the structure and energy of covalent systems," Phys Rev B, vol. 37, pp. 6991–7000.

[15] Brenner, D.W., 1990, "Empirical potential for hydrocarbons for use in simulating the chemical vapor deposition of diamond films," Phys Rev B, vol. 42, pp. 9458–9471.

[16] Xiao, T., Liao, K., 2002, "Nonlinear elastic properties of carbon nanotubes subjected to large axial deformations," Phys Rev B, vol. 66, pp. 153407–153410.

[17] Yu, M. F., Lourie, O., Dyer, M. J., Mploni, K., Kelly, T. F., Ruoff, R. S., 2000, "Strength and breaking mechanism of multiwall carbon nanotubes under tensile load," Science, 287, pp. 637–640.

[18] Bozovic, D., Bockrath, M., 2003, "Plastic deformations in mechanically strained single-walled carbon nanotubes," Phys Rev B, vol. 67, pp. 33407–33410.

[19] Allen, M. P., Tildesley, D. J., 1987, "Computer simulation of liquids," Oxford: Clarendon Press.

[20] Frenkel D. , Smit B., 1996, "Understanding molecular simulation from algorithms to applications," Academic Press Inc. USA.

[21] Yeak, S. H., Ng, T. Y. , Liew, K. M., 2005, "Multiscale modeling of carbon nanotubes under axial tension and compression," Phys. Rev. B, vol. 72, pp. 165401-165404.

[22] Chowdhury, S.C., Okabe, T., 2007, "Computer simulation of carbon nanotube pull-out from polymer by the molecular dynamics method," Composites: Part A, 38, pp.747–754.